Natural Convection from a Vertical Wavy Surface Embedded in Saturated Porous Media

S. U. Rahman*,† and H. M. Badr‡

Departments of Chemical and Mechanical Engineering, King Fahd University of Petroleum & Minerals, Dhahran-31261, Kingdom of Saudi Arabia

The mass-transfer coefficients have been obtained experimentally for natural convection from vertical wavy surfaces of varying amplitude-to-wavelength ratio (a/λ) when embedded in saturated porous media. The porous media were formed by randomly packing glass spheres of 3-, 4-, and 6-mm diameters. A limiting diffusion current technique based on cathodic reduction of cupric ions in acidic solution was used. The obtained data correspond to high Rayleigh numbers and exhibit non-Darcian effects. The mass-transfer coefficients from the wavy surfaces in porous media can be estimated as $Sh_L^* = [3.3284 - 2.4068(a/\lambda)](Ra_L^*/Da_L)^{0.26}$ in the studied range of Ra_L^* $[(1.31 \times 10^6) - (5.56 \times 10^7)]$, where Ra_L^* and Da_L are the modified Rayleigh and Darcy numbers, respectively.

1. Introduction

During the past two decades, there has been increasing interest in the study of natural convection from straight and wavy heated surfaces embedded in porous media. The engineering applications of these studies are numerous, including, for example, thermal insulation of buildings, nuclear waste disposal, thermal analysis of petroleum reservoirs, design of grain storage containers, and many others. The problem of natural convection from straight surfaces embedded in porous media has received more attention because of its simple geometry and the very many related applications. Comprehensive reviews of the work done on this problem have been published by Nield and Bejan[1] and Ingham and Pop.[2] The following literature search focuses on the problem of natural convection from wavy surfaces.

The problem of natural convection from a vertical wavy surface placed in a Newtonian fluid was investigated by Moulic and Yao[3] for the special case of a uniform heat flux. The investigation was based on a step-by-step numerical integration of the steady governing equations of motion and energy after transformation to boundary-layer coordinates following the work by Yao.[4] The method of solution was flexible enough to tackle a wavy surface of any shape. The results showed that the local and average Nusselt numbers were uniformly smaller than those of a flat plate because of the thicker velocity and thermal boundary layers. It was also found that the wavelength of the variation of the total Nusselt number is half that of the wavy surface and the amplitude decays downstream. Chiu and Chou[5] carried out a numerical investigation of the problem of transient natural convection from a semi-infinite vertical wavy surface placed in a micropolar fluid of infinite extent. The transient flow and thermal fields were due to sudden heating of the wavy surface. It was found that increasing the amplitude/wavelength ratio results in increasing the velocity and thermal boundary-layer thickness, leading to a decrease in the local and average heat-transfer rates. In comparison with a Newtonian fluid, the micropolar fluid resulted in a lower heat-transfer rate and larger skin friction.

Rees and Pop[6] obtained a similarity solution for the problem of free convection along an isothermal vertical wavy surface placed in a porous medium. By using a generalized similarity transformation, they showed that the governing boundary-layer equations could be reduced to those of a vertical flat surface obtained by Cheng and Minkowicz[7] in cases of very high Rayleigh numbers. An analytical expression was obtained for the local Nusselt number variation in terms of the Rayleigh number and the distance from the leading edge. It was also shown that the local Nusselt number is less than or equal to that of a plane surface because of the thicker boundary layer. Rees and Pop[8] revisited the same problem but considered the special case of uniform heat flux. The equations of motion were exactly the same, and the changes were only in the boundary conditions. After introducing three transformations and letting $Ra \rightarrow \infty$, they solved the resulting boundary-layer equations numerically using the Keller box method. Results were obtained for wavy surfaces with amplitudes of the same order of magnitude as the wavelength and for very high Rayleigh numbers. Local hot spots were found in similar places on the wavy surface, and the analysis was restricted to values of x that are O(1) as $Ra \rightarrow \infty$.

The problem of laminar natural convection from a horizontal wavy surface was investigated by Murthy et al.[9] The surface represents the lower side of a two-dimensional rectangular enclosure that is filled with a fluid-saturated porous medium. The enclosure had two adiabatic vertical walls and two isothermal horizontal ones. The study was based on a numerical solution of the fluid flow and heat-transfer equations using finite elements. It was found that the heat flux decreases with increasing wavy surface amplitude. Moreover, an increase of the Rayleigh number caused marginal changes in heat transfer. The streamline and isotherm patterns were only reported in the low-Ra range (from 25 to 100). In comparison with the case of a flat wall, the wavy wall resulted in less heat transfer. Kumar et al.[10] studied

* Corresponding author. E-mail: srahman@kfupm.edu.sa.
† Department of Chemical Engineering.
‡ Department of Mechanical Engineering.

10.1021/ie020143p CCC: $22.00
Published on Web 07/24/2002

Table 1. Geometrical Details[a] of the Wavy Surfaces

data point	surface 1 $\lambda = 1.99$ cm, $2a = 0.20$ cm, $a/\lambda = 0.050$			surface 2 $\lambda = 1.99$ cm, $2a = 0.40$ cm, $a/\lambda = 0.103$			surface 3 $\lambda = 2.00$ cm, $2a = 0.58$ cm, $a/\lambda = 0.144$			surface 4 $\lambda = 2.01$ cm, $2a = 0.79$ cm, $a/\lambda = 0.198$		
	L (cm)	P (cm)	A (cm^2)	L (cm)	P (cm)	A (cm^2)	L (cm)	P (cm)	A (cm^2)	L (cm)	P (cm)	A (cm^2)
1	0.50	0.51	0.66	0.498	0.55	0.70	0.50	0.59	0.76	0.50	0.67	0.85
2	1.00	1.02	1.32	0.995	1.09	1.41	1.00	1.18	1.53	1.01	1.32	1.70
3	1.49	1.53	1.97	1.493	1.64	2.11	1.50	1.78	2.29	1.51	1.98	2.55
4	1.99	2.04	2.63	1.990	2.18	2.82	2.00	2.37	3.05	2.01	2.64	3.40
5	2.49	2.55	3.29	2.488	2.73	3.52	2.50	2.958	3.82	2.51	3.30	4.25
6	2.99	3.06	3.95	2.985	3.28	4.23	3.00	3.55	4.58	3.02	3.95	5.10
7	3.48	3.57	4.603	3.48	3.82	4.93	3.50	4.14	5.34	3.52	4.61	5.95
8	3.98	4.08	5.261	3.98	4.37	5.64	4.00	4.73	6.10	4.02	5.27	6.80
9	4.48	4.59	5.919	4.48	4.91	6.34	4.50	5.32	6.87	4.52	5.93	7.65

[a] Here, L = vertical length from the leading edge, P = profile length corresponding to L., A = mass-transfer area ($L \times P$).

natural convection in a rectangular enclosure having three flat walls and one wavy vertical wall. The enclosure was filled with a porous medium and heated from the wavy wall side. The two vertical walls were isothermal, whereas the two horizontal walls were thermally insulated. The equations of motion and energy were solved numerically using finite elements following the work by Murthy et al.[9] The results indicated that the global heat flux increases with increasing *Ra* but decreases with increasing amplitude. The global rate of heat transfer was found to decrease with increasing number of waves, and in all cases, the heat transfer was less than that of a flat surface. The loss of global heat flux was attributed to the loss in the convection-favoring vertical component of the buoyancy force.

Kim[11] obtained a numerical solution for the problem of natural convection from a wavy vertical isothermal plate to a non-Newtonian fluid with emphasis on the effects of flow index, Prandtl number, and surface geometry. The results showed that, with an increase in flow index, the axial velocity increases, and the velocity boundary layer becomes thinner. The local heat-transfer coefficient was found to be high at the starting point on the vertical surface but to decrease downstream. The thermal boundary layer of pseudo-plastic fluids was found to be thinner than that of dilatant fluids. The wavelength of the local Nusselt number was half that of the wavy surface, and the effects of amplitude decreased in the downstream direction. Finally, the local Nusselt number was found to decrease with increasing amplitude of the surface. Recently, Rahman[12] conducted an experimental study of natural convection from a vertical wavy surface to a Newtonian fluid with the objective of obtaining the mass-transfer coefficients. The surfaces considered were sinusoidal with varying amplitude-to-wavelength ratio (a/λ). The study revealed that the rate of mass transfer decreases with increasing a/λ. A correlation for the Sherwood number was obtained in terms of the Rayleigh number and a/λ for the Raleigh number range from 2.3×10^8 to 1.9×10^{11}.

This work represents an experimental investigation of natural convection from a vertical wavy surface embedded in a fluid-saturated porous medium. From the above literature search, it is clear that all of the work done on this problem has been mainly theoretical with no experimental verification of the obtained results.

2. Experimental Section

The mass-transfer coefficients were measured using the limiting diffusion current technique (LDCT). In this technique, the potential difference between the working electrode (object for which mass-transfer coefficient is desired) and an auxiliary electrode is varied, and the current densities are recorded when the electrodes are in a suitable electrolyte system. For each hydrodynamic situation, the limiting current density is obtained from current density vs potential plots. At the limiting condition, the rate of reaction essentially equals the rate of mass transfer. Therefore

$$N_A = k_L(C_b - C_s) = \frac{i_L}{zF} \tag{1}$$

Because $C_s = 0$ under these conditions, the mass-transfer coefficient can be estimated by

$$k_L = \frac{i_L}{zFC_b} \tag{2}$$

The mass-transfer coefficient in eq 2 is the average value over the studied vertical length L. In principle, any electrode−electrolyte system can be utilized for this purpose, provided that a nonreactive supporting electrolyte is used to minimize the contribution due to migration current. For this work, the reduction of copper ions in acidic cupric sulfate solution was chosen. This system was selected for its well-defined limiting current plateau.[13] A solution of 0.618 M $CuSO_4$ and 3.09 M H_2SO_4 was prepared. The concentrations of $CuSO_4$ and H_2SO_4 were determined through idiometric and acid−base titrations, respectively.

Sinusoidal wavy surfaces were machined from solid copper blocks. Four different surfaces of varying amplitude/wavelength (a/λ) ratios were prepared. Their amplitudes varied from 1 to 4 mm while the wavelength remained constant at 20 mm. This resulted in values of $a/\lambda = 0.05$, 0.1, 0.15, and 0.20 approximately. The geometrical details of the wavy surfaces are given in Table 1. Eight surfaces were fabricated for each a/λ ratio. The thickness of each sample was 10 mm, and the width was 12.9 mm. A copper wire was gas-welded at one end of the sample for electrical connections. The machined wavy surfaces were prepared by application of increasing grades of emery paper (100, 400, 600, and 1500 grit size) and finally by washing with acetone to remove any oil/grease. The surface was covered by an insulating paint so that only the area on which mass-transfer coefficients were desired was exposed. A sample prepared in this manner functioned as a working electrode and was inserted in the packed bed. The packed bed was formed in a 1-L cylindrical vessel with 3-, 4-, or 6-mm glass spheres. The porosities of the packing materials were determined by the water re-

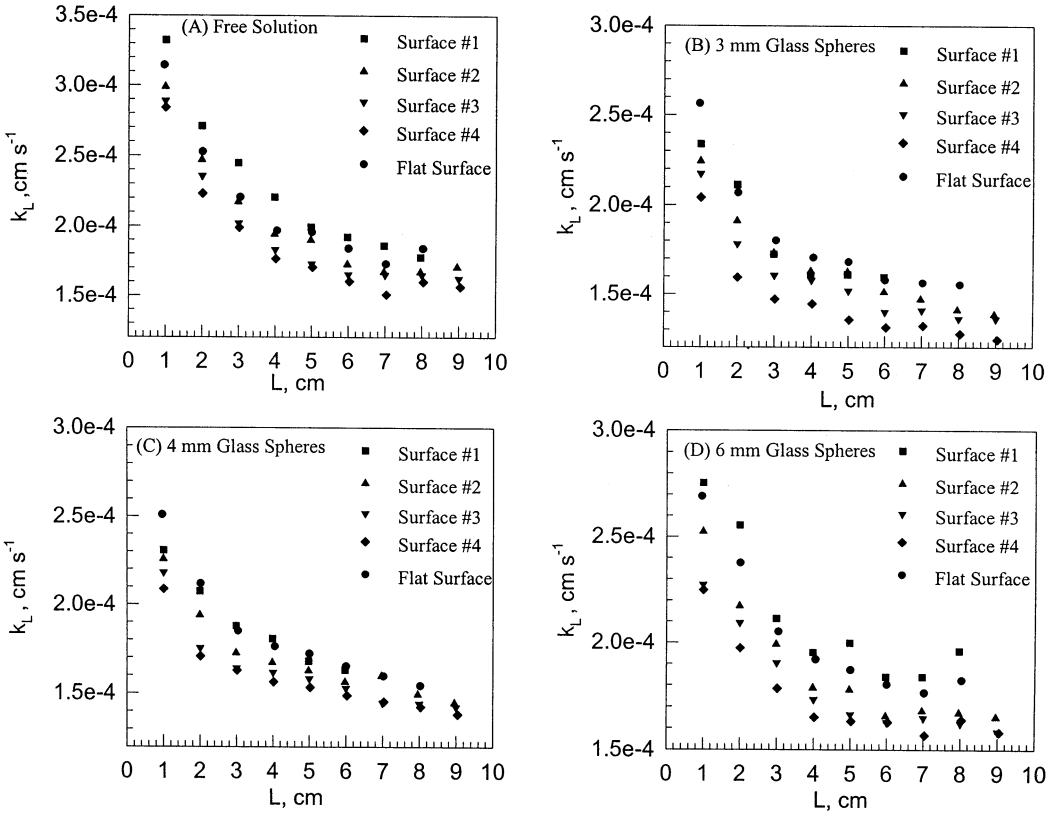

Figure 1. Variation of average mass transfer with vertical distance of various wavy surfaces in (A) free solution, (B) saturated packing of 3-mm glass spheres, (C) saturated packing of 4-mm glass spheres, and (D) saturated packing of 6-mm glass spheres.

placement method. The packing material was saturated with the described electrolyte. The verticality of the working electrode was ensured by using a spirit level.

A copper cylinder, kept inside the bed near the wall, was used as the counter electrode. A saturated calomel electrode was embedded in the bed to function as a reference electrode. The temperature was measured by a thermometer of 0.1 °C precision. The working, counter, and reference electrodes were connected to a potentiostat (model 273A, EG&G PARC). The potentiostat was driven by software (model 352, EG&G PARC) via a microcomputer. Potentiostatic linear polarization curves were obtained for all wavy surfaces embedded in different packing materials and suspended in free solution. The experimental setup is shown elsewhere.[17]

3. Data Reduction

The polarization curves obtained for a wavy surface in free solution or embedded in porous media exhibit pronounced limiting current plateaus between 450 and 650 mV SCE. The limiting currents determined from these curves were used to calculate the average mass-transfer coefficients (k_L) from eq 2. The physicochemical properties of the acidic cupric sulfate solution that are required to calculate Sherwood and Rayleigh numbers were estimated from a temperature-dependent empirical correlation given by Chiang and Goldstein.[14] The density of the solution at the surface (ρ_o) is also needed to evaluate Rayleigh number. Its evaluation necessitates an estimation of the concentrations of H_2SO_4 and $CuSO_4$ at the surface. For mass-transfer-controlled regime, the surface concentration of $CuSO_4$ can be taken as zero, and the concentration of H_2SO_4 can be calculated by utilizing principle of electroneutrality and the correlation given by Selman and Tobais.[13]

Table 2. Ranges of Various Parameters in This Study

parameter	range
particle diameter, mm	3.0−6.0
temperature, °C	21.6−24.6
porosity	0.371−0.417
permeability, cm^2	(4.69×10^{-4})−(2.45×10^{-3})
Sc	3776−4369
Ra_L^*	(1.31×10^6)−(5.56×10^7)
a/λ	0.050−0.198

The following relation estimates the effective mass diffusivity for a given media from the molecular diffusivity

$$D_e = \frac{D\epsilon}{\tau} \tag{3}$$

where τ is the tortuousity of the porous media. The recommended value[151] of τ for regular packing materials is 4. The permeability of the medium is estimated using Carman−Kozeny's equation[1]

$$K = \frac{d_p^{\,2}\epsilon}{180(1-\epsilon)^2} \tag{4}$$

4. Results and Discussion

When an undulated surface is embedded in a saturated porous medium, two factors influence natural convection, namely, the surface geometry (a/λ) and the porous nature of the medium. The experimental observations of these two factors are discussed in this section, and the ranges of the parameters are given in Table 2.

4.1. Effect of Undulations. The average mass-transfer coefficients obtained for all four wavy surfaces and for a flat surface are plotted for different packing

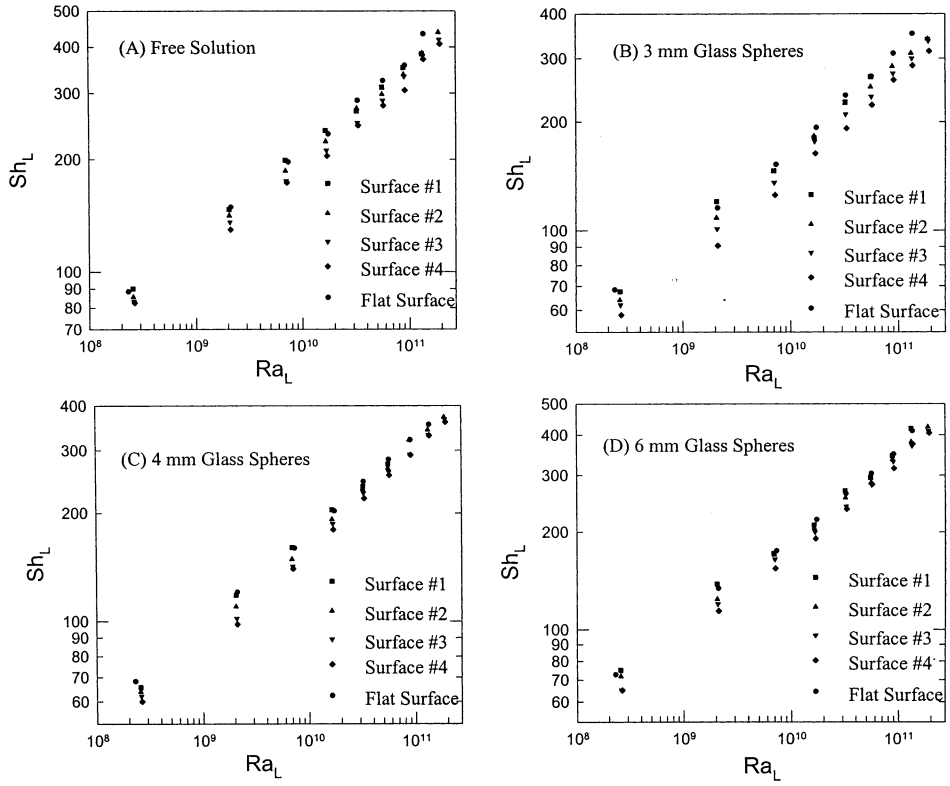

Figure 2. Variation of average Sherwood number with Rayleigh number of various wavy surfaces in (A) free solution, (B) saturated packing of 3-mm glass spheres, (C) saturated packing of 4-mm glass spheres, and (D) saturated packing of 6-mm glass spheres.

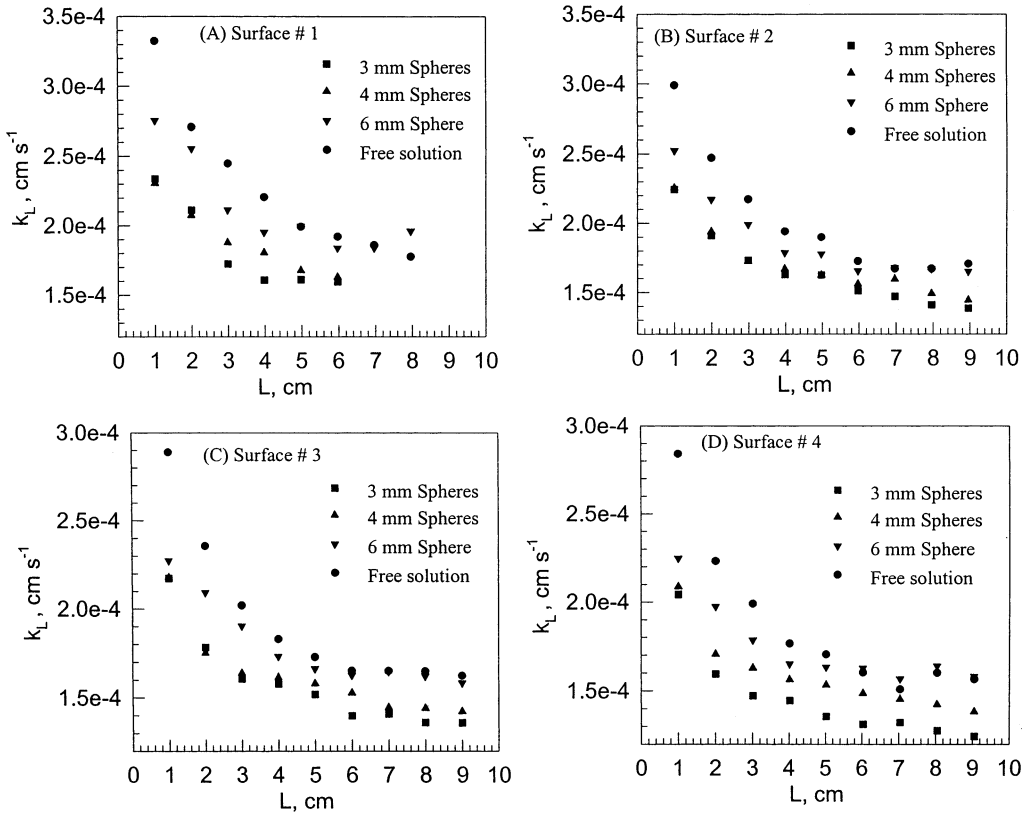

Figure 3. Variation of average mass transfer with vertical distance in various porous media for (A) surface 1, (B) surface 2, (C) surface 3, and (D) surface 4.

materials and for free solution (i.e., without packing) in Figure 1. In general, all of these plots show that the mass-transfer coefficient decreases with vertical distance from the bottom edge (L), conforming to the predictions of boundary-layer theory. The mass-transfer coefficients also decrease with increasing a/λ ratio. However, the dependency of k_L on L cannot be established on the basis of these plots, as the temperature was not constant during the experimentation. To eliminate the effect of temperature, it is necessary to replot

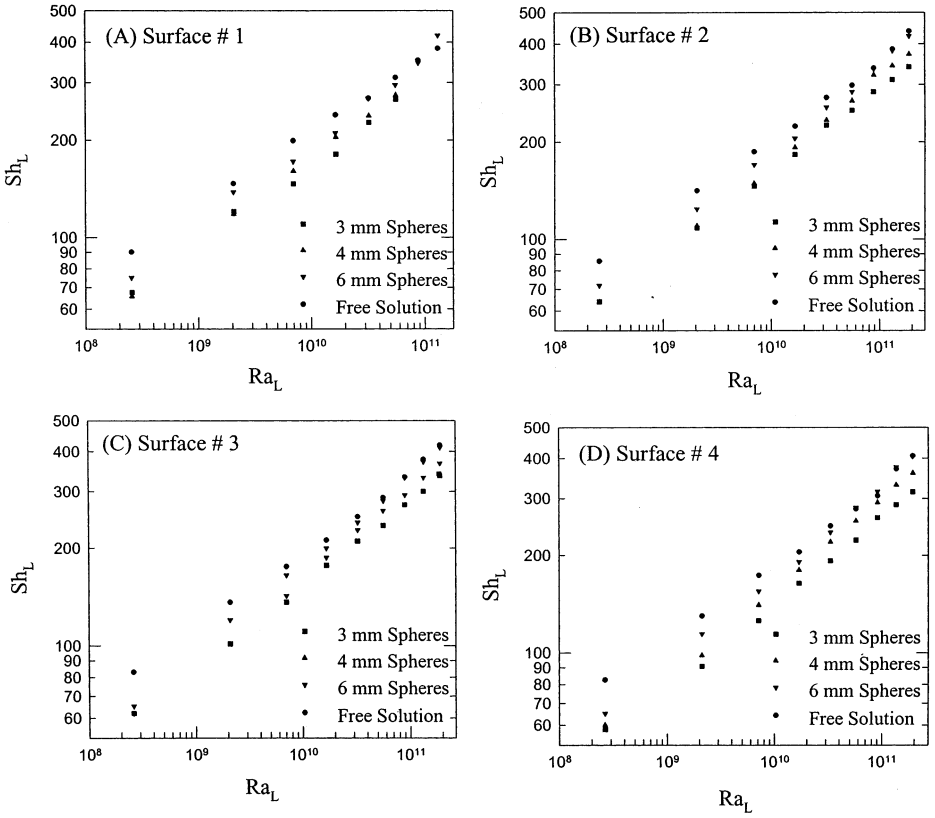

Figure 4. Variation of average Sherwood number with Rayleigh number in various porous media for (A) surface 1, (B) surface 2, (C) surface 3, and (D) surface 4.

data using dimensionless quantities, (i.e., Sh_L and Ra_L). This is done in Figure 2. It is interesting to note that the Sh_L values for the flat surface and for surface 1 ($a/\lambda = 0.05$) are almost same, indicating that, for smaller a/λ, the waviness of the surface does not significantly influence the mass transfer. This inference is consistent in all packing materials. Nevertheless, Sh_L decreases with increasing a/λ for free solution as well as for all packing materials.

A vertical wavy surface is composed of infinite inclined surfaces of varying inclination angle (θ) whose value changes from $-\theta_o$ to θ_o. Here, θ_o is a function of a/λ. The inclination angle is 0 at the troughs and crests, whereas at the nodes, its value is $-\theta_o$ or θ_o. When cos(θ) equals 1 (i.e., at a trough or a crest), the effect of gravity reaches a maximum, and the component of fluid velocity parallel to the surface is highest. This situation is identical to that of a flat vertical surface, and therefore, the local boundary layer thickness and the heat- and mass-transfer coefficients will also be identical. However, at nodes [where cos(θ) is a minimum], the corresponding values will be smallest. This results in lower average heat- and mass-transfer coefficients. It should also be noted that θ_o will be large for larger a/λ values for the surface. Therefore, the average heat- and mass-transfer coefficients will be smaller for a surface with larger a/λ. The same conclusions can be drawn from Figure 2.

4.2. Effect of Packing Material. To elucidate the effect of the packing material, the average mass-transfer coefficients are plotted against vertical length for all packing materials and for free solution, as shown in Figure 3. The mass-transfer coefficients seem to decrease with decreasing diameter of the packing glass spheres. The scatter in these plots is due to variations in the ambient temperature. The nondimensional parameters (Sh_L and Ra_L) were estimated using physicochemical properties calculated at the actual temperatures of the experiments. The resulting values of Sh_L are plotted against Ra_L in Figure 4. The effect of packing material is more visible and consistent in these plots. It is evident that the average Sherwood number depends on the size of the packing material, which manifests itself in terms of permeability. It is known that the permeability increases with the size of packing spheres.[1]

In the literature pertaining to transport in saturated media, the data are normally presented in terms of modified Rayleigh and Sherwood numbers estimated using the effective diffusivity (D_e)

$$Ra_L^* = \frac{gKL(\rho/\rho_o - 1)}{\nu D_e} \tag{5}$$

$$Sh_L^* = \frac{k_L L}{D_e} \tag{6}$$

Kim and Vafai[16] mathematically modeled heat transfer from flat vertical surfaces in saturated porous media and obtained the following relation between Sh_L^* and Ra_L^*

$$Sh_L^* = 0.785\left(\frac{Ra_L^*}{Da_L}\right)^{0.25} \tag{7}$$

where Da_L is the Darcy number, defined as

$$Da_L = \frac{K}{\epsilon L^2} \tag{8}$$

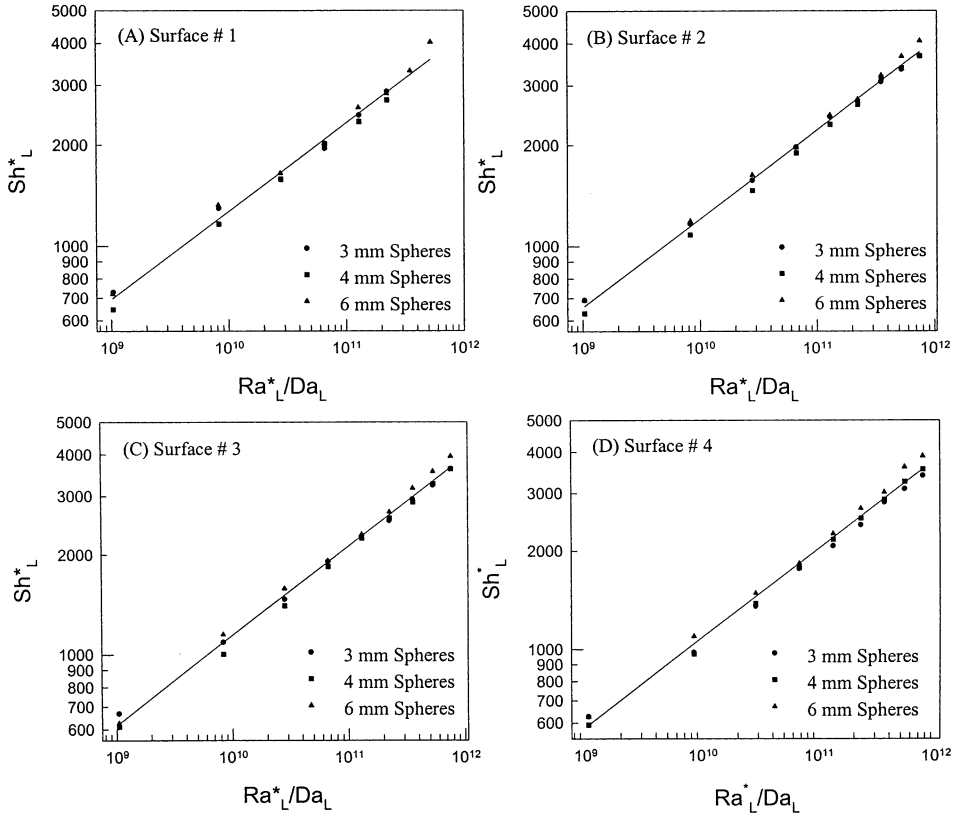

Figure 5. Variation of average modified Sherwood number (Sh_L^*) with Ra_L^*/Da_L for (A) surface 1, (B) surface 2, (C) surface 3, and (D) surface 4.

For vertical flat surfaces embedded in porous media, Rahman et al.[17] obtained an equation to predict Sh_L^* in similar form

$$Sh_L^* = 3.32\left(\frac{Ra_L^*}{Da_L}\right)^{0.26} \tag{9}$$

The data from the present study are plotted as Sh_L^* versus Ra_L^*/Da_L in Figure 5. In each of these plots, data for all packing materials are regressed into a power law equation. The resulting equations, with values of the corresponding correlation coefficients, are given as follows:

For surface 1

$$Sh_L^* = 3.043(Ra_L^*/Da)^{0.262} \qquad R^2 = 0.9886 \tag{10}$$

For surface 2

$$Sh_L^* = 2.757(Ra_L^*/Da)^{0.264} \qquad R^2 = 0.9950 \tag{11}$$

For surface 3

$$Sh_L^* = 2.367(Ra_L^*/Da)^{0.268} \qquad R^2 = 0.9945 \tag{12}$$

For surface 4

$$Sh_L^* = 2.067(Ra_L^*/Da)^{0.272} \qquad R^2 = 0.9920 \tag{13}$$

It can be noted that the effect of undulation is perceptible in both of the regression coefficients. The constant decreases from 3.32 (for a flat surface) to 3.043, 2.757, 2.367, and 2.067 for wavy surfaces of increasing a/λ. Similarly, the power of the correlation (eqs 9−13) increases from 0.26 (in the case of a flat surface) to 0.262, 0.264, 0.268, and 0.272 for increasing intensity of undulations.

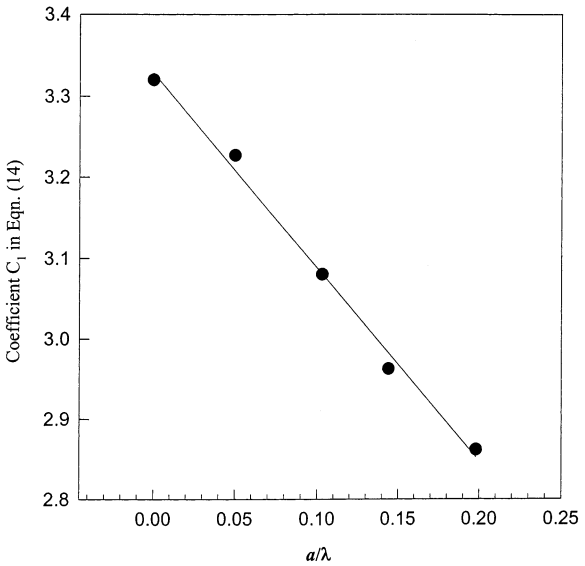

Figure 6. Coefficient C_1 of eq 14 versus a/λ.

In an effort to obtain an explicit expression for Sh_L^* in terms of Ra_L^*, Da_L, and a/λ, the data were replotted as Sh_L^* versus $(Ra_L^*/Da_L)^{0.26}$ and fitted to straight lines. This resulted in the equation

$$Sh_L^* = C_1\left(\frac{Ra_L^*}{Da_L}\right)^{0.26} \tag{14}$$

The value of the coefficient C_1 is plotted against a/λ in Figure 6. The curve could be fitted to the following

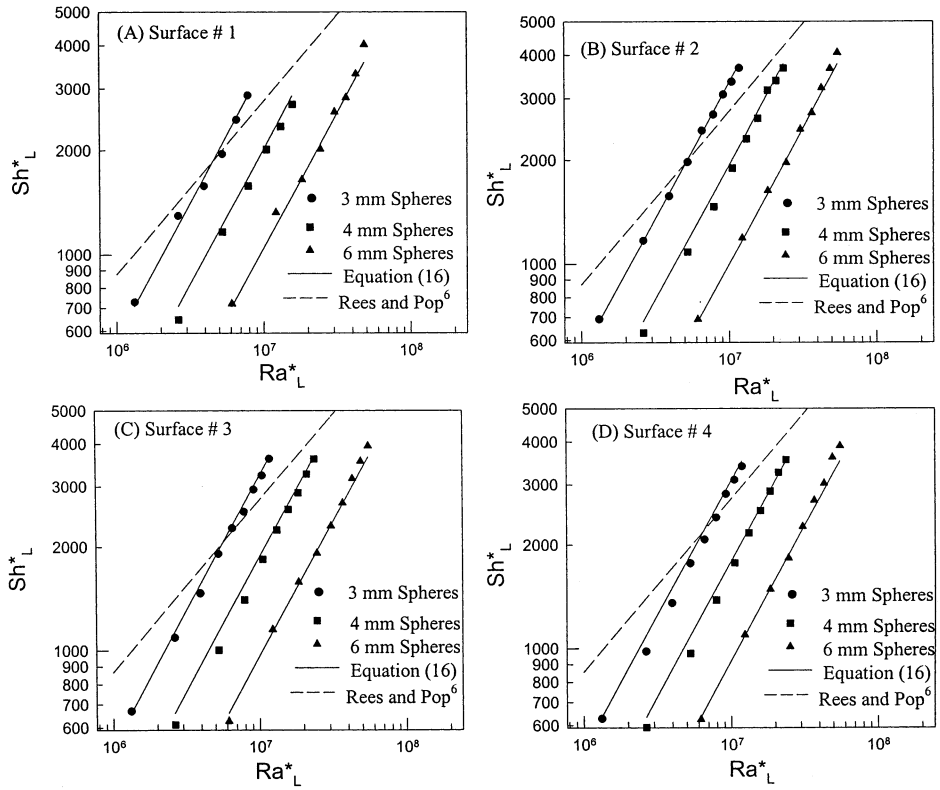

Figure 7. Experimental and predicted values of Sh_L^*.

straight line with $R^2 = 0.996$

$$C_1 = 3.3284 - 2.4068\left(\frac{a}{\lambda}\right) \tag{15}$$

By substituting the value of C_1 from eq 15 into eq 14, an explicit equation for natural convective mass transfer from wavy surfaces embedded in saturated porous materials can be obtained as

$$Sh_L^* = \left[3.3284 - 2.4068\left(\frac{a}{\lambda}\right)\right]\left(\frac{Ra_L^*}{Da_L}\right)^{0.26} \tag{16}$$

Equation 16 predicts the mass-transfer coefficients with an average error of 4%. The experimental data as well as eq 16 are plotted in Figure 7 for each wavy surface. The plots exhibit excellent agreement between eq 16 and the experimental data.

Rees and Pop[6] obtained a similarity solution for the problem in question using Darcy's equation. The mass-transfer counterpart of their result is written as

$$Sh_x^* = \frac{0.444(Ra_x^*)^{0.5}}{\sqrt{1 + [(a/\lambda)\cos(x/\lambda)]^2}} \tag{17}$$

The values averaged over the length L can be found by integrating eq 17 from $x = 0$ to $x = L$, resulting in

$$Sh_L^* = 0.443\,75\sqrt{\frac{Ra_L^*}{L}}\int_0^L \frac{dx}{\sqrt{x\{1 + [(a/\lambda)\cos(x/\lambda)]^2\}}} \tag{18}$$

It is interesting to note that eq 18 reduces to the Cheng and Mincowycz[7] equation for vertical flat surfaces embedded in porous media for $a/\lambda = 0$. The Sherwood numbers predicted by eq 18 are plotted in Figure 7 along with eq 16. The mismatch is apparent, and eq 18 does not distinguish between various particle sizes. This is mainly because of the Darcian flow assumption, which is only valid for low values of Raleigh numbers ($Ra_L^* < 5000$). As the particle diameter of the porous medium increases, non-Darcian effects become more significant. This behavior is in agreement with natural convection from vertical flat surfaces in porous media.[17]

5. Conclusions

Natural convection mass-transfer coefficients from wavy copper surfaces held vertical in free acidic cupric sulfate solution and in saturated porous media were obtained. The limiting diffusion current technique (LDCT) based on cupric ion deposition was used. The following conclusions can be drawn on the basis of the obtained data: (a) In free solution, the mass-transfer coefficients of wavy surfaces are less than that of a vertical flat surface. (b) The mass-transfer coefficient decreases with increasing a/λ ratio. (c) The mass-transfer coefficient for a flat surface embedded in saturated porous medium is less than that for a vertical flat surface in free solution. A similar inference can be made for wavy surfaces of a given a/λ ratio. (d) The deterioration of mass-transfer coefficients is high in less permeable media. (e) In a porous medium of given permeability, the mass-transfer coefficients decrease with increasing (a/λ) ratio. (f) The average Sherwood number from a wavy surface embedded in a saturated porous medium can be predicted by eq 16 within the studied range of parameters.

Nomenclature

a = amplitude of the wavy surface (cm)
A = mass-transfer area (cm^2)

C_b = bulk concentration of cupric ions (mol/L)
C_s = surface concentration of cupric ions (mol/L)
D = diffusivity of copper ions in acidic copper sulfate solution (cm^2/s)
Da_L = Darcy number, $K/\epsilon L^2$
D_e = effective diffusivity, eq 3
d_p = particle diameter
F = Faraday's constant
g = acceleration due to gravity (cm/s^2)
i_L = limiting current (mA)
K = permeability, eq 3
k_L = average mass-transfer coefficient (cm/s)
L = vertical distance (cm)
Pr = Prandtl number
Ra_L = average Rayleigh number, $gL^3(\rho_\infty/\rho_o - 1)/\nu D$
Ra_L^* = average modified Rayleigh number, $gKL(\rho/\rho_o - 1)/\nu D_e$
Sc = Schmidt number, ν/D
Sh_L = Average Sherwood number, $k_L L/D$
Sh_L^* = average Sherwood number estimated with effective diffusivity, $k_L L/D_e$
z = number of electrons in the reduction reaction

Greek Letters

ρ = density of the bulk solution (g/cm^3)
ρ_o = density of the solution at the surface (g/cm^3)
ν = kinematic viscosity (cm^2/s)
θ = local inclination angle of the wavy surface
θ_o = maximum value of θ
λ = wavelength of the wavy surface (cm)
ϵ = porosity
τ = tortuosity
μ = viscosity (P)

Literature Cited

(1) Nield, D. A.; Bejan, A. *Convection in Porous Media*, 2nd ed.; Springer-Verlag: New York, 1999.

(2) Pop, I.; Ingham, D. B.; Merkin, J. H. Transient Convection Heat Transfer in a Porous Medium: External Flows. In *Transport Phenomena in Porous Media*; Ingham, D. B., Pop, I., Eds.; Elsevier Science: New York, 1998.

(3) Moulic, S. G.; Yao, L. S. Natural Convection Along a Vertical Wavy Surface with Uniform Heat Flux. *ASME J. Heat Transfer* **1989**, *111*, 1106.

(4) Yao, L. S. A Note on Prandtl's Transposition Theorem. *ASME J. Heat Transfer* **1988**, *110*, 507.

(5) Chiu, C. P.; Chou, H. M. Transient Analysis of Natural Convection Along a Vertical Wavy Surface in Micropolar Fluids. *Int. J. Eng. Sci.* **1994**, *32* (1), 19.

(6) Rees, D. A.; Pop, I. A Note on Free Convection Along a Vertical Wavy Surface in a Porous Medium. *ASME J. Heat Transfer* **1994**, *116*, 505.

(7) Cheng, P.; Minkowicz, W. J. Free Convection About a Vertical Flat Plate Embedded in a Porous Medium with Application to Heat Transfer from a Dike. *J. Geophys. Res.* **1977**, *82*, 2040.

(8) Rees, D. A.; Pop, I. Free Convection Induced by a Vertical Wavy Surface with Uniform Heat Flux in a Porous Medium. *ASME J. Heat Transfer* **1995**, *117*, 547.

(9) Murthy, P. V.; Kumar, B. V.; Singh, P. Natural Convection Heat Transfer from a Horizontal Wavy Surface in a Porous Enclosure. *Num. Heat Transfer A* **1997**, *31*, 207.

(10) Kumar, B. V.; Singh, P.; Murthy, P. V. Effect of Surface Undulations on Natural Convection in a Porous Square Cavity. *ASME J. Heat Transfer* **1997**, *119*, 848.

(11) Kim, E. Natural Convection Along a Wavy Vertical Plate to Non-Newtonian Fluids. *Int. J. Heat Mass Transfer* **1997**, *40* (11), 3069.

(12) Rahman, S. U. Natural Convection Along Vertical Wavy Surfaces: An Experimental Study. *Chem. Eng. J.* **2001**, *84*, 587.

(13) Selman, J. R.; Tobais, C. W. Mass Transfer Measurements by Limiting Current Technique. *Adv. Chem. Eng.* **1981**, *10*, 211.

(14) Chiang, H. D.; Goldstein, R. J. Application of the Electrochemical Mass Transfer Technique to the Study of Buoyancy-Driven Flows. In *Transport Phenomena in Heat and Mass Transfer*; Reizes, J. A., Ed.; Elsevier: New York, 1991; Vol. 1, pp 1−25.

(15) Smith, J. M. *Chemical Engineering Kinetics*; McGraw-Hill International Book Company: New York, 1981.

(16) Kim, S. J.; Vafai, K. Analysis of Natural Convection about a Vertical Plate Embedded in Porous Medium. *Int. J. Heat Mass Transfer* **1989**, *32* (4), 665.

(17) Rahman, S. U.; Al-Saleh, M. A.; Sharma, R. N. Experimental Investigation of Natural Convection from Vertical Surface Embedded in Saturated Porous media. *Ind. Eng. Chem. Res.* **2000**, *39*, 214.

Received for review February 19, 2002
Revised manuscript received June 5, 2002
Accepted June 20, 2002

IE020143P